

## Chemistry and mineralogy of wood-tin, Black Range, New Mexico

JOHN L. LUFKIN

*Department of Geological Sciences, The University of Texas at Austin  
Austin, Texas 78712*

### Abstract

Wood-tin occurs as placer accumulations at several localities in the Black Range, southwestern New Mexico. Individual nuggets, 3 cm or less in diameter, commonly enclose fragments of porphyritic rhyolite, and contain cassiterite, hematite, cristobalite, and/or chalcedony. Color zoning is well developed in wood-tin and appears to have chemical significance; the iron content in cassiterite-rich layers, as much as 7.8 percent  $\text{Fe}_2\text{O}_3$  by electron probe analysis, generally increases through the color sequence: tan, yellow, red, dark brown. The addition of iron is correlated with a decrease in both the  $c$  cell parameter and the cell volume of cassiterite, suggesting that  $\text{Fe}^{3+}$  has substituted for  $\text{Sn}^{4+}$  in the crystal structure. Although wood-tin is rarely found as lode deposits, it probably was deposited originally as fracture fillings in the Tertiary Taylor Creek rhyolite with which it is closely associated. A low temperature, low pressure environment of deposition is reasonable for the wood-tin.

### Introduction

Wood-tin, a term generally applied to sub-microscopic to finely crystalline, concentrically-layered cassiterite, occurs as placer accumulations in eluvial and alluvial gravels in the Black Range tin district of southwestern New Mexico. Rarely, it is observed *in situ* as fracture fillings in the Taylor Creek rhyolite of Tertiary age (Fig. 1) that forms flow-domes exposed just west of the Continental Divide in Sierra and Catron Counties (Fries, 1940; Fries and Butler, 1943; Lufkin, 1972). Based on estimates of the U.S. Bureau of Mines (Volin *et al.*, 1947), production of tin concentrates from the district during World War II was about 10 long tons, averaging 50 per cent tin. Since 1970, small mining operations have shipped approximately 40 short tons of wood-tin concentrate averaging about 61 percent tin from the vicinity of Hardcastle Creek (Frank Gitman, oral communication). The following account is based on petrographic, X-ray, and electron probe studies of more than twenty specimens collected by the writer and Professor R. H. Jahns from eluvial gravels and jig concentrates in Sawmill Canyon, Hardcastle Creek, and Squaw Creek.

The Black Range wood-tin typically occurs in Holocene gravel deposits as isolated nuggets, generally less than 3 cm in diameter, although fist-sized specimens have been observed. It seems highly probable that the wood-tin was precipitated originally as

veinlets in the Taylor Creek rhyolite which is exposed over an area of 177 kms<sup>2</sup>. Almost half of the material studied has cores or inclusions of altered and re-placed rhyolite, and the placer deposits are closely associated spatially with outcrops of Taylor Creek rhyolite. At Squaw Creek, a small amount of wood-tin has been observed in place as fracture fillings in this rhyolite.

### Mineralogy

Wood-tin nuggets are rarely composed of pure cassiterite. Other mineral phases present include, in order of decreasing abundance, hematite, cristobalite, and chalcedony. Cristobalite and chalcedony are much less abundant, and commonly absent from many nuggets. The typical colloform texture suggests sequential encrustations of these minerals on walls of fractures. Many of the nugget cores consist of altered porphyritic rhyolite with a groundmass that is divitrified to aggregates of fine-grained quartz and alkali feldspar. These rhyolite inclusions are typically elongate and as much as 18 mm long by 4 mm wide. The cusped or botryoidal depositional pattern of wood-tin adjacent to the rhyolite contact commonly reflects small irregularities in the planar to slightly convex rhyolite surface. In places, the rhyolite groundmass is replaced by fine-grained, disseminated to colloform cassiterite, with phenocrysts of quartz and sanidine left intact. In one specimen, quartz, sanidine, and

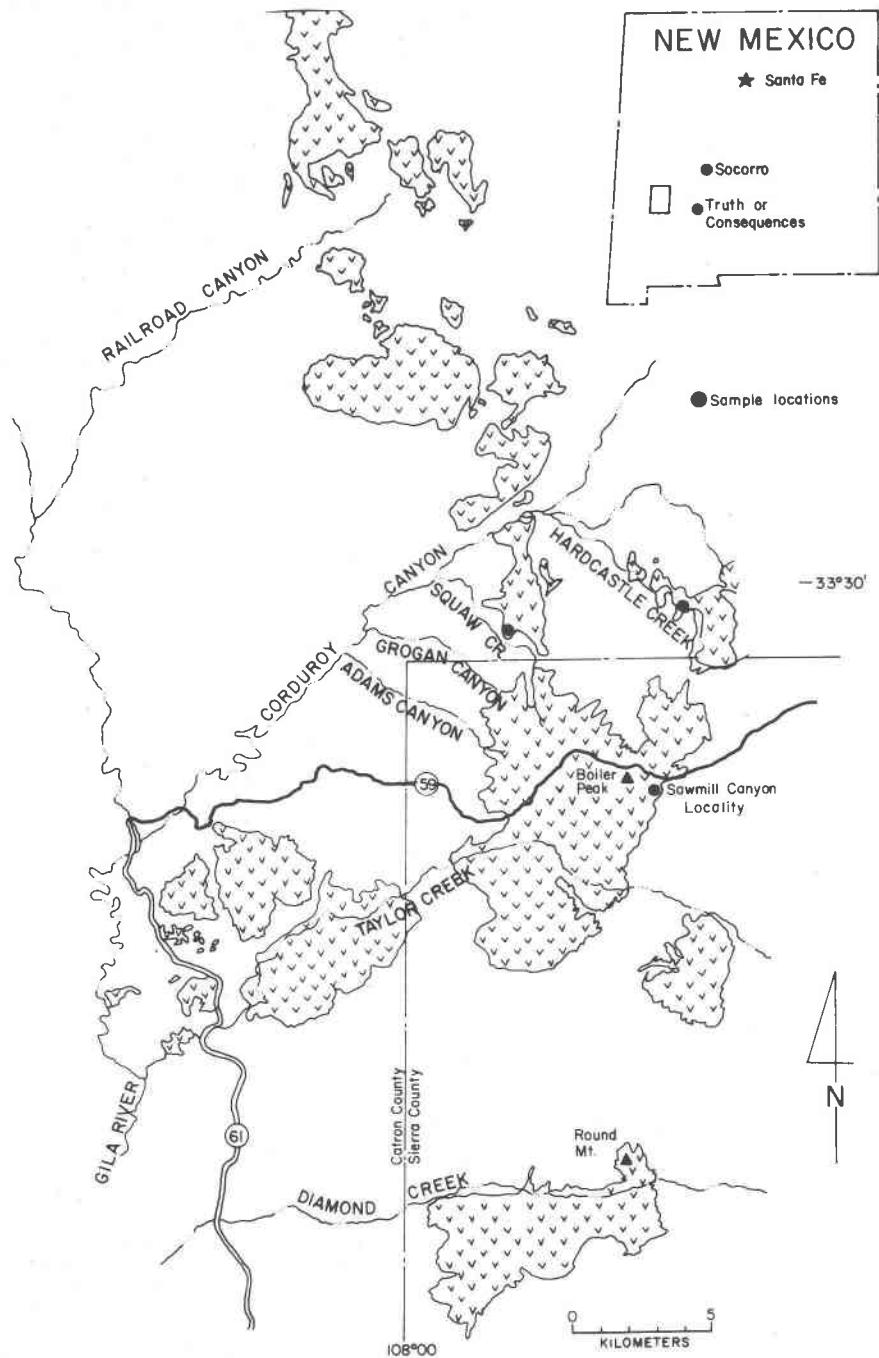


Fig. 1. Map showing outcrop distribution of the Taylor Creek rhyolite and sample locations of wood-tin examined in this study. After Fries and Butler (1943).

topaz(?) were present in the groundmass of the rhyolite core, but not in the body of the surrounding wood-tin nugget.

Proceeding outward from the rhyolite core, the body of the wood-tin nuggets is composed primarily of microcrystalline cassiterite, with lesser amounts of

hematite, cristobalite, and/or chalcedony. Cassiterite varies in size from microcrystalline aggregates to elongate crystals, 2.2 mm long; much of the cassiterite is present as elongated, radial grains a few microns in length. There does not appear to be any systematic variation in grain size, although cassiterite tends to be

coarser grained in the rhyolite inclusions and in peripheral shells of the nodules. Color variations in cassiterite help to define the colloform texture of wood-tin. In transmitted light, cassiterite displays shades of tan, gray, yellow, orange, red, and brown, or is opaque. Less commonly, it is almost colorless. Where opaque, cassiterite generally contains abundant inclusions of hematite. In reflected light, cassiterite appears dull gray with low reflectivity in air. There is a general correspondence between color and crystal layering, but in coarser-grained layers, color boundaries may depart from crystal outlines, or terminations. Slight pleochroism is noted, but only in the larger crystals.

Hematite ranges from minute particles to plates of specularite, 2.8 mm wide. In the altered rhyolite inclusions hematite is disseminated, but throughout the

body of wood-tin it generally occurs in layers and varies in shape from radial, needle-like crystals to more equant grains. Less commonly, it forms semi-circular masses of radiating crystals. The distribution of hematite-rich layers is non-uniform; most of the hematite is deposited in areas adjacent to the nugget interiors, suggestive of an early formation. However, some nuggets also feature hematite in their peripheral shells as well.

Where present, cristobalite and less commonly, chalcedony, form thin shells, 0.4 mm or less thick, on the wood-tin surfaces. Cristobalite occurs in equigranular mosaics or is fibrous, and the X-ray diffraction pattern of this material matches that of low cristobalite. In one specimen, cristobalite occurs as linear, mosaic aggregates interlayered with cassiterite. Portions of these mosaic patches are optically continuous, possibly suggestive of inversion to the more stable alpha quartz. Chalcedony is the least abundant constituent of wood-tin. It typically forms a thin, light-colored coating on the nodules.

### Chemistry

Nine wood-tin nodules were chemically analyzed by electron probe. Traverses were made across individual nuggets from rim to core to determine their purity and to see if the various colors of the cassiterite layers had chemical significance. Analyses for  $\text{SnO}_2$  and  $\text{Fe}_2\text{O}_3$  were determined for several differently colored layers of cassiterite in each specimen, excluding grains of other minerals. A beam diameter of 2–10 microns was employed. Due to the generally submicroscopic textures developed in wood-tin, grain boundaries of cassiterite generally could not be resolved in polished section during probe analysis.

Probe analyses of wood-tin are presented in Table 1. With the exception of specimens 18 and 21, most of the analyzed cassiterite consists of aggregates of tiny crystals a few microns long. Specimens 18 and 21 have larger grains, 2.2 mm or less in length. The  $\text{SnO}_2$  and  $\text{Fe}_2\text{O}_3$  analyses of the micron-size cassiterite do not total 100 percent, whereas those of the coarser grained material do. As an independent check, relatively pure wood-tin practically identical to specimen 2 was submitted to the Gulf Chemical and Metallurgical Company for wet chemical analysis. The partial analysis is:  $\text{SnO}_2$ , 97.17;  $\text{Fe}_2\text{O}_3$ , 0.43;  $\text{SiO}_2$ , 0.77. By comparison, the probe analysis for  $\text{SnO}_2$  in specimen 2 is almost 3 percent less than the wet chemical analysis of similar material, while the iron content is about the same. The explanation for the low totals of probe analyses, particular  $\text{SnO}_2$ , probably is related

Table 1. Electron probe analyses of wood-tin, Black Range, New Mexico

Specimen No.	$\text{SnO}_2$	$\text{Fe}_2\text{O}_3^*$	Color of cassiterite†
2	94.3	0.3	tan
8	92.6	0.7	colorless
	86.2	3.2	yellow-green brown
	84.6	4.4	yellow brown
	86.8	5.9	orange brown
9	86.5	5.3	yellow brown
	86.5	6.9	red brown
10	90.5	1.6	tan
	91.5	1.6	yellow
	89.9	1.7	light brown
	88.1	2.5	yellow orange
	91.8	2.7	red orange
11	93.1	2.5	yellow brown
	91.6	3.7	yellow
	91.6	4.2	orange red
	90.3	4.5	yellow brown
	89.5	5.3	dark brown
12	96.1	0.8	tan
	91.6	2.5	yellow
	91.6	2.6	brown
	90.9	5.8	red
	86.8	5.8	dark brown
13	90.7	5.0	brown orange
	94.0	5.3	red orange
	89.4	7.8	yellow orange
18	101.5	0.2	colorless
	101.3	0.5	yellow orange
	100.6	0.4	orange
21	99.9	1.0	yellow
	96.9	2.1	orange
	96.8	2.8	red brown

\*Total Fe as  $\text{Fe}_2\text{O}_3$ .

†Color based on observations of wood-tin in thin section, transmitted light.

to the fine-grained texture of wood-tin and micro-pore spaces along grain boundaries (which are observed in thin-section of specimen 2, but generally not in other material). This suggestion is compatible with the results obtained on single crystals in specimens 18 and 21, where a complete probe analysis is obtained for tin and iron alone. Therefore, it seems unlikely that other major elements are present in significant concentration in wood-tin. Where analyzed,  $\text{SiO}_2$  and  $\text{Al}_2\text{O}_3$  are present in amounts generally less than 0.5 percent combined. Trace elements present in wood-tin, determined by microprobe wave length scans and X-ray fluorescence, include As, Cl, Pb, Zn, Ag, In, and S.

From the chemical data, it is apparent that there is a general correlation between cassiterite color and its iron content. With few exceptions, the iron content in cassiterite-rich layers increases progressively through the color sequence: colorless, tan or light brown, yellow, orange, red, and dark brown (Fig. 2). However, the iron content cannot be accurately predicted from the color. Cassiterite of similar color may vary by several percent  $\text{Fe}_2\text{O}_3$  between different nuggets. For example, yellow cassiterite may contain from 1 to 2.5 percent  $\text{Fe}_2\text{O}_3$ , red cassiterite, 4 to 6 percent, and red brown varieties, 3 to 7 percent  $\text{Fe}_2\text{O}_3$ . Factors that may affect the accuracy of color correlation with

composition include variations in texture, porosity, and mineral thickness from specimen to specimen.

Much study has been devoted to color zoning in coarse-grained cassiterite of deep-seated vein and pegmatite affiliations, but very little on the finer grained wood-tin occurrences of volcanic origin. The red color in some New Zealand cassiterites has been attributed to tantalum (Hutton, 1950), although it was not determined whether the tantalum was present in the crystal structure or as inclusions of tantalum-bearing minerals. Some colored cassiterites, typically brown to black, have been related to ferrous iron content (Greaves *et al.*, 1971; Leube and Stumpfl, 1963; Pecora *et al.*, 1950). Color in cassiterites from Aberfoyle, Tasmania, zoned in shades of brown, red, and black, apparently cannot be correlated with iron content, but the deep red zones contain higher values of Mn and Nb compared with pale brown zones of the same crystal (Edwards and Lyon, 1957).

Other investigations suggest that there is no relation between color and chemical composition in cassiterite. Noll (1948, in Leube and Stumpfl, 1963), in his study of largely European tin deposits, considered color to be related to submicroscopic exsolution bodies. In their microprobe study of zoned cassiterite crystals from Pelepah Kanan, Johore, Grubb and

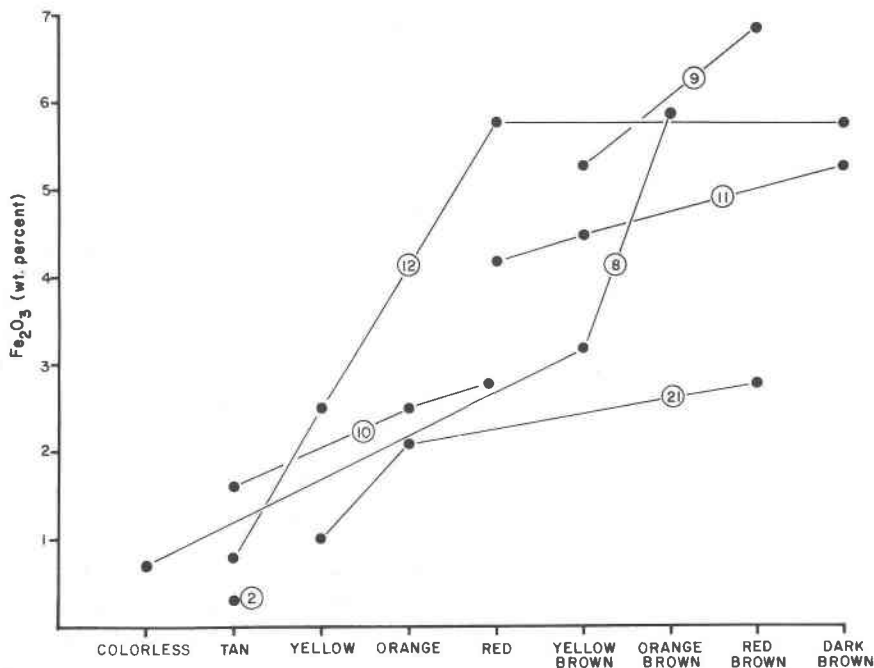


Fig. 2. Scatter diagram showing the relationship between color of wood-tin and its iron content. Specimen numbers correspond to those presented in Table 1.

Hannaford (1966) observed that some light-colored zones contained more iron than dark-colored, magnetic zones. Gotman (1938, in Singh and Bean, 1968) concluded from research of Russian tin occurrences that color and light absorption of cassiterite are in part due to changes in the state of the crystal lattice under diverse conditions of formation and also to the presence of various impurities. Ta and Nb, common in cassiterite from pegmatites, may replace Sn, causing a disturbance in valency balance and lattice of cassiterite.

The first attempt to explain color variations in wood-tin was probably by Newhouse and Buerger (1928). In their petrographic study of several specimens from Mexico and the western United States, including the Black Range, they correlated the cassiterite color to proximity of hematite, noting that cassiterite tends to be a deeper red adjacent to hematite grains. If iron is the principal pigmenting agent in the Black Range wood-tin, as indicated from this microprobe study, it could be present either as finely divided iron oxide inclusions or incorporated in the cassiterite structure as  $\text{Fe}^{2+}$ ,  $\text{Fe}^{3+}$ , or both. Because

hematite was the only iron oxide identified by X-ray and polished-section study, it is reasonable to assume, without the aid of Mössbauer spectra, that the iron in cassiterite is dominantly  $\text{Fe}^{3+}$ . Several standard mineralogy texts state that  $\text{Fe}^{3+}$  may proxy for  $\text{Sn}^{4+}$  in cassiterite. Cations of comparable size and charge that may substitute for tin as well include  $\text{Ti}^{4+}$ ,  $\text{Nb}^{5+}$ ,  $\text{Ta}^{5+}$ , and  $\text{Sc}^{3+}$ . This latter group of elements, however, was not detected in this investigation.

To evaluate the possibility of  $\text{Fe}^{3+}$  substitution for  $\text{Sn}^{4+}$  in the cassiterite lattice, six powdered specimens of wood-tin of different color and Fe content were mounted separately on a polycrystalline silicon disc, which provided an internal standard. A Phillips X-ray diffractometer was employed, using Cu radiation, a graphite reflected beam monochromator, and a scanning speed of  $0.25^\circ/\text{minute}$ . Lattice reflections were measured between  $60$  and  $116$  degrees  $2\theta$ , and were used in a least-squares refinement of the cell constants. Cell dimensions of these specimens are recorded in Table 2 and compared with data of Swanson and Tatge (1953). The Fe-bearing cassiterites

Table 2. Unit-cell dimensions of cassiterite in wood-tin, Black Range, New Mexico\*

Specimen No.	a (Å)	c (Å)	V (Å <sup>3</sup> )	Fe <sub>2</sub> O <sub>3</sub> (wt. percent)
2	4.7342(6)	3.1835(5)	71.35(2)	0.3
17	4.733(1)	3.1833(9)	71.30(4)	n.a.
22	4.7341(7)	3.1828(9)	71.33(2)	n.a.
5	4.734(2)	3.177(3)	71.21(7)	n.a.
9	4.736(2)	3.173(3)	71.16(7)	5.3-6.9
13	4.730(5)	3.177(4)	71.1(1)	5.0-7.8
2763	4.738	3.188	71.566	

n.a. - not analyzed.

2. Tan to beige cassiterite, very fine grained.  
 17. Cream colored cassiterite, very fine grained.  
 22. Tan to beige cassiterite, similar to No. 2.  
 5. Orange-red cassiterite, coarse grained.  
 9. Yellow-brown to red-brown cassiterite, very fine grained.  
 13. Red-orange to orange-brown cassiterite, fine grained.  
 2763. SnO<sub>2</sub>, National Bureau of Standards (Swanson and Tatge, 1953).

\*The estimated standard deviation given in parentheses refers to the last decimal position.

(nos. 5, 9, and 13) consistently feature a smaller  $c$  cell edge and a smaller cell volume,  $V$ ; the  $a$  cell dimension, however, does not seem to vary systematically. A decrease in cell volume would be expected with  $\text{Fe}^{3+}$  substitution, since the  $\text{Fe}^{3+}$  ion is smaller than  $\text{Sn}^{4+}$  (0.63 Å and 0.67 Å radii in 6-fold coordination, respectively; Shannon and Prewitt, 1969, p. 943).

Diffraction patterns of Fe-bearing and Fe-poor cassiterites from the wood-tin nuggets were compared with that obtained from an unanalyzed single cassiterite crystal, Lost River, Alaska. The general appearance of the peaks suggests that the wood-tin cassiterite is not as well crystallized and that the Fe-bearing cassiterite (no. 9) features broader and less defined reflections—a situation that might be expected if Fe were present in the cassiterite structure.

### Discussion and conclusions

Wood-tin placers are widespread in the Black Range, but are closely associated with the Taylor Creek rhyolite, which contains small amounts of hematite and non-colloform cassiterite in veinlets at several localities. This relationship, together with the common presence of rhyolite inclusions in wood-tin nodules, indicates that the wood-tin was deposited originally as veinlets in the Taylor Creek rhyolite. The general absence of lode wood-tin suggests that most of the colloform cassiterite was deposited in stratigraphically higher sections of the rhyolite that were subsequently eroded.

The initial environment of wood-tin deposition is conjecture. Similarities of these deposits to the Mexican tin-bearing rhyolites bespeak a similar origin and environment. Heating and recrystallization experiments performed on Mexican wood-tin (Pan and Ypma, 1973, 1974) appear to favor a low-temperature (<150°C) genesis, although the substitutional effects of Fe for Sn on the stability of cassiterite have not yet been investigated. Concentration and precipitation of tin oxide in volcanic rocks suggests low pressure as well (close to 1 atm). The chemistry and mineralogy of wood-tin nodules implies that the mineralizing fluids contained appreciable iron and silica, in addition to tin. Zoning in wood-tin and cell refinements of cassiterite suggest further that most of the iron was precipitated early as  $\text{Fe}^{3+}$  in both the structures of hematite and cassiterite. Most of the silica was deposited later in the paragenetic sequence as cristobalite and chalcedony.

The colloform and botryoidal texture that characterizes wood-tin has been widely attributed to colloidal processes since the turn of the century. Nod-

ules of Black Range wood-tin, however, feature both colloform and isolated crystals of cassiterite in the same section, suggesting that the colloform texture is but one size range, albeit very fine grained, in a continuum, as pointed out by Roedder (1968). Rapid nucleation promoted by highly saturated solutions (not necessarily colloidal) may well account for these fine-grained textures that are so common in silica, carbonates, and iron and manganese oxide minerals.

The chemical stability of cassiterite in the zone of weathering is generally recognized, although it may alter to the soft, hydrous oxide of tin, varlamoffite (Alexander and Flinter, 1965; Singh and Bean, 1968). Secondary cassiterite may form in the oxidized zone of tin sulfide deposits, apparently by alteration of stannite (e.g. Ramdohr, 1969). Considering the stability of cassiterite, the absence of sulfides, and the lack of supergene enrichment in the exposed tin-bearing veinlets in the district, the precipitation of wood-tin from hypogene rather than supergene solutions is favored.

### Acknowledgments

This investigation was funded in part by a grant from the University Research Institute, The University of Texas at Austin (U.R.I. Project SRF-628). I thank Professor R. H. Jahns (Stanford University) who kindly provided me with additional wood-tin material, C. L. Sainsbury and G. A. Desborough (U.S. Geological Survey) for their gift of high-purity cassiterite that was used as a tin standard in the microprobe work, and Drs. J. Hoggins and H. Steinfink, Department of Chemical Engineering, for their valuable assistance with the cell refinement work. This manuscript has benefited from the reviews of A. W. Laughlin, R. C. Ewing, and D. S. Barker. The Geology Foundation, The University of Texas at Austin, gave financial support for the publication of this article.

### References

- Alexander, J. B. and B. H. Flinter (1965) A note on varlamoffite and associated minerals from the Batang Padang district, Perak, Malaya, Malaysia. *Mineral. Mag.*, 35, 622–627.
- Edwards, A. B. and R. J. P. Lyon (1957) Mineralization at Aberfoyle tin mine, Rossarden, Tasmania. *Australia Inst. Min. Metall.*, 181, 93–145.
- Fries, C., Jr. (1940) Tin deposits of the Black Range, Catron and Sierra Counties, New Mexico, a preliminary report. *U.S. Geol. Survey Bull.*, 922-M, 355–370.
- and A. P. Butler (1943) Geologic map of the Black Range tin district, New Mexico. U.S. Geol. Survey open-file map.
- Greaves, G., B. G. Stevenson and R. G. Taylor (1971) Magnetic cassiterite from Herberton, North Queensland, Australia. *Econ. Geol.*, 66, 480–487.
- Grubb, P. L. C. and P. Hannaford (1966) Ferromagnetism and colour zoning in some Malayan cassiterite. *Nature*, 209, 677–678.
- Hutton, C. O. (1950) Studies of heavy detrital minerals. *Bull. Geol. Soc. Am.*, 61, 635–716.
- Leube, A. and E. F. Stumpf (1963) The Rooiberg and Leeuport

- tin mines, Transvaal, South Africa. Part 2. Petrology, mineralogy and geochemistry. *Econ. Geol.*, 58, 527-557.
- Lufkin, J. L. (1972) *Tin Mineralization within Rhyolite Flow-domes, Black Range, New Mexico*. Ph.D. Thesis, Stanford University, Stanford, California.
- Newhouse, W. H. and M. J. Buerger (1928) Observations on wood-tin nodules. *Econ. Geol.*, 23, 185-192.
- Pan, Y. and P. J. M. Ypma (1973) The Mexican type tin deposit—its occurrence, chemistry and physical conditions of deposition (abstr.). *Geol. Soc. Am. Abstr. Progr.*, 5, 762.
- (1974) Heating and recrystallization of wood-tin—an indication of low temperature genesis of cassiterite and wood-tin veins in volcanics (abstr.). *Geol. Soc. Am. Abstr. Progr.*, 6, 62-63.
- Pecora, W. T., G. Switzer, A. L. Barbosa and A. T. Myers (1950) Structure and mineralogy of the Golconda pegmatite, Minas Gerais, Brazil. *Am. Mineral.*, 35, 889-901.
- Ramdohr, P. (1969) *The Ore Minerals and their Intergrowths*. Pergamon Press, Oxford. 1174 p.
- Roedder, E. (1968) The non-colloidal origin of "colloform" textures in sphalerite ores. *Econ. Geol.*, 63, 451-471.
- Shannon, R. D., and C. T. Prewitt (1969) Effective ionic radii in oxides and fluorides. *Acta Crystallogr.*, B25, 925-946.
- Singh, D. S. and J. H. Bean (1968) Some general aspects of tin minerals in Malaysia. In, *A Technical Conference on Tin*, Vol. 2. Int. Tin Council, London. p. 457-478.
- Swanson, H. E. and E. Tatge (1953) Standard X-ray diffraction powder patterns. *Natl. Bur. Stand. Circ.* 539, Vol. 1, 54-55.
- Volin, M. E., P. L. Russell, F. L. C. Prive and D. H. Mullen (1947) Catron and Sierra Counties tin deposits, New Mexico. *U.S. Bur. Mines Rept. Inv.* 4068, 60 p.

*Manuscript received, January 14, 1976; accepted  
for publication, August 5, 1976.*

## Electron diffraction study of phase transformations in copper sulfides

ANDREW PUTNIS

*Department of Mineralogy and Petrology, University of Cambridge  
Downing Place, Cambridge CB2 3EW, England*

### Abstract

The order-disorder transformation behavior of chalcocite and djurleite, and digenite and anilite has been studied by direct observations of the transformations in a transmission electron microscope. Chalcocite and djurleite represent low-temperature superstructures of the high-temperature disordered chalcocite subcell, and there need be no compositional difference between them. The djurleite superstructure is the more stable form at room temperature. The intermediate structure in digenite forms through modulated structures rather than through twinning. A metastable *6a* digenite type superstructure, isochemical with anilite, forms on heating. This *6a* superstructure is metastable relative to the formation of anilite.

### Introduction

For compositions near  $\text{Cu}_2\text{S}$  a number of phases are known to exist at room temperature. These may be divided into two broad categories based on the nature of the sulfur close-packing in the structure: (1) chalcocite and djurleite with structures based on hexagonal close-packing of sulfur atoms; (2) digenite-like structures and anilite with sulfur atoms in approximately cubic close-packing. The low-temperature phase relations have been summarized by Morimoto and Gyobu (1971) and Barton (1973). The transformation behavior of some of these phases and the relationships between them have been studied by direct observation of the transformations in a transmission electron microscope.

### Method

Naturally-occurring crystals of the phases were crushed, after chilling in liquid nitrogen to prevent deformation. The finest grains were collected from a suspension in absolute alcohol and mounted on a standard carbon-coated copper grid for observations in an AEI EM6G transmission electron microscope operating at 100kV. Observations were made firstly on untransformed grains by using a small condenser aperture and a defocussed beam to keep the illumination and the heating effect of the beam minimal. Transformations in the grains, both on heating and cooling, can be observed by focussing and defocussing the beam or by moving the beam laterally on and off the grain. Although the temperature in the grain

cannot be directly measured in this way, the course of a transformation can be followed dynamically, and subtle changes which would be very difficult to observe by X-ray methods can clearly be seen.

### I: The transformation behavior of chalcocite and djurleite

Chalcocite is generally considered to have a composition very close to  $\text{Cu}_2\text{S}$ , whereas djurleite, originally thought to be  $\text{Cu}_{1.97}\text{S}$  (Roseboom, 1966; Takeda *et al.*, 1967a) is now considered to be a solid solution with a composition range from about  $\text{Cu}_{1.93}\text{S}$  to  $\text{Cu}_{1.97}\text{S}$  (Mathieu and Rickert, 1972; Potter, 1974).

The phases and cell dimensions of chalcocite and djurleite may be summarized as follows. Between  $104^\circ$  and  $435^\circ\text{C}$  chalcocite is hexagonal with  $a_h = 3.95$ ,  $c_h = 6.75 \text{ \AA}$  and space group  $P6_3/mmc$ . Above  $435^\circ\text{C}$  it has the cubic close-packed digenite structure. Below  $104^\circ\text{C}$  a pseudo-orthorhombic cell with  $a = 11.92$ ,  $b = 27.34$ ,  $c = 13.44 \text{ \AA}$ , space group  $Ab2m$  is formed (Buerger and Buerger, 1944). This can be described as a superstructure of the hexagonal form with  $a = 3a_h$ ,  $b = 4\sqrt{3}a_h$ ,  $c = 2c_h$ . More recently it has been shown that low-chalcocite is monoclinic (Evans, 1971), but the pseudo-orthorhombic cell will be used here for convenience.

Djurleite is orthorhombic, diffraction aspect  $P^*n^*$  with cell dimensions  $a = 26.90$ ,  $b = 15.72$ ,  $c = 13.57 \text{ \AA}$ . The diffraction aspect is also compatible with the monoclinic space group  $P2_1/n$ . Takeda *et al.* (1967a) point out that these cell dimensions are closely re-